Parasite Immunology

WILEY

Parasite Immunology

ORIGINAL ARTICLE OPEN ACCESS

Unveiling the Role of Endoplasmic Reticulum Stress Pathways in Canine Demodicosis

Pamela A. Kelly[1] | Gillian P. McHugo[2] | Caitriona Scaife[3] | Susan Peters[1] | M. Lynn Stevenson[4] | Jennifer S. McKay[5] | David E. MacHugh[2,6] | Irene Lara Saez[7] | Rory Breathnach[1]

[1]UCD School of Veterinary Medicine, University College Dublin, Dublin 4, Ireland | [2]UCD School of Agriculture and Food Science, University College Dublin, Dublin 4, Ireland | [3]Proteomics Core, Mass Spectrometry Resource, UCD Conway Institute of Biomolecular and Biomedical Research, University College Dublin, Dublin 4, Ireland | [4]School of Biodiversity, One Health and Veterinary Medicine, Bearsden, University of Glasgow, Glasgow, UK | [5]IDEXX Laboratories, Wetherby, UK | [6]UCD Conway Institute of Biomolecular and Biomedical Research, University College Dublin, Dublin 4, Ireland | [7]UCD Charles Institute of Dermatology, University College Dublin, Dublin 4, Ireland

Correspondence: Pamela A. Kelly (pamela.kelly@ucd.ie)

Received: 17 August 2023 | **Revised:** 29 February 2024 | **Accepted:** 8 March 2024

Funding: This work was supported by the UCD Wellcome Institutional Strategic Support Fund, which was financed jointly by University College Dublin and the SFI-HRB-Wellcome Biomedical Research Partnership (Ref. 204844/Z/16/Z). G.P.M. is supported by an SFI Investigator Award (Grant No. SFI/15/IA/3154).

Keywords: canine demodicosis | *Demodex* | eIF2 signalling | endoplasmic reticulum stress | M2 macrophages | unfolded protein response

ABSTRACT

Canine demodicosis is a prevalent skin disease caused by overpopulation of a commensal species of *Demodex* mite, yet its precise cause remains unknown. Research suggests that T-cell exhaustion, increased immunosuppressive cytokines, induction of regulatory T cells and increased expression of immune checkpoint inhibitors may contribute to its pathogenesis. This study aimed to gain a deeper understanding of the molecular changes occurring in canine demodicosis using mass spectrometry and pathway enrichment analysis. The results indicate that endoplasmic reticulum stress promotes canine demodicosis through regulation of three linked signalling pathways: eIF2, mTOR, and eIF4 and p70S6K. These pathways are involved in the modulation of Toll-like receptors, most notably TLR2, and have been shown to play a role in the pathogenesis of skin diseases in both dogs and humans. Moreover, these pathways are also implicated in the promotion of immunosuppressive M2 phenotype macrophages. Immunohistochemical analysis, utilising common markers of dendritic cells and macrophages, verified the presence of M2 macrophages in canine demodicosis. The proteomic analysis also identified immunological disease, organismal injury and abnormalities and inflammatory response as the most significant underlying diseases and disorders associated with canine demodicosis. This study demonstrates that *Demodex* mites, through ER stress, unfolded protein response and M2 macrophages contribute to an immunosuppressive microenvironment, thereby assisting in their proliferation.

1 | Introduction

Canine demodicosis is a prevalent skin disease commonly seen in primary care small animal practice [1, 2]. It occurs when a species of the commensal skin mite *Demodex* genus overpopulates the skin [3]. There are three identified species of *Demodex* mites reported in dogs, with the most common being *Demodex canis* [2, 4]. The other species include *Demodex injai* and *Demodex cornei*; the latter is a likely variant of *D. canis* [5–8]. The disease is clinically classified based on lesion location and extent (generalised, localised) and/or age of onset (juvenile onset—less than 18 months of age and adult onset—greater than 4 years of age) [1, 2]. The adult-onset disease is typically linked with concurrent illnesses

or treatments that cause immunosuppression, such as neoplasia, endocrinopathies and corticosteroid administration [2, 3, 9, 10].

The exact pathogenesis of canine demodicosis is not yet fully understood. The leading hypothesis is of immune dysregulation and T-cell exhaustion, with dogs with demodicosis having increased expression of immunosuppressive cytokine IL-10, decreased expression of IL-2, IL-21 and reduced circulating CD4+ cells. This hypothesis is supported by the high incidence of demodicosis in dogs with immunosuppressive diseases or undergoing immune modulating therapy [2, 4, 10–12]. However, there are instances where there is no evidence of immunosuppression, and in these cases, appropriate antiparasitic treatment leads to recovery and limited relapse [2, 9, 13–15]. With these cases, it is hypothesised that the *Demodex* mite itself is modulating the immune response. Research has shown that TLR2 expression is high in cases of canine demodicosis, and it is thought to be one of the main contributing causes of the high levels of IL-10. Recently, it has been demonstrated that regulatory T cells, known to produce IL-10, are increased in the skin of dogs with demodicosis in comparison with control skin samples from healthy canines. Increased gene expression of several immune checkpoint molecules including PD-1/PD-L1 and CTLA-4 has also recently been shown in cases of canine demodicosis [16]. These findings support the possibility that the *Demodex* mites could induce changes in the hair follicle, sebaceous gland and/or immune cells that promote immune tolerance and support its proliferation.

Research into the pathogenesis of canine demodicosis has mainly focused on mRNA expression changes in both blood and tissue, with only a few studies exploring changes at the protein level using immunohistochemistry and flow cytometry [13, 14, 17–27]. Protein-level studies have primarily focused on assessing a limited panel of proteins such as cytokines and cell receptors [17–19, 21, 23]. Proteomics is a crucial technology in human medicine for understanding disease pathogenesis, discovering biomarkers and identifying potential treatment targets [28]. Proteomics offers advantages over conventional genomics and transcriptomics tools as it can detect post-translational modifications like phosphorylation, glycosylation and acetylation, providing a deeper characterisation of skin diseases' pathogenesis [29]. Currently, there are limited proteomic profiling studies reported in veterinary medicine for skin diseases.

The aim of this study was to enhance our understanding of the molecular changes occurring in canine demodicosis. To achieve this, we examined the proteomic profile of formalin-fixed paraffin-embedded (FFPE) skin samples of dogs with canine demodicosis using mass spectrometry (MS) and compared them with profiles from control skin samples. Additionally, we aimed to characterise the dendritic cell and macrophage population in lesional skin from dogs with demodicosis using immunohistochemical analysis.

2 | Methods

2.1 | Proteomics

2.1.1 | Case Selection

This study obtained ethical exemption from the Animal Research Ethics Committee (AREC) at University College Dublin (AREC E 19 09 Kelly).

Ten FFPE skin samples from dogs diagnosed histologically with canine demodicosis were selected. Five of these samples were from dogs with juvenile-onset demodicosis (i.e., dogs younger than 18 months) and five were from dogs with adult-onset demodicosis (i.e., dogs older than 4 years). All 10 had skin swabs for microbiological assessment taken on the day of biopsy sampling, of which culture results were considered 'normal skin flora'. 'Normal skin flora' is considered when culture is of normal commensal skin bacteria, which includes Gram-positive staphylococci, *Corynebacterium* spp., viridans streptococci, *Micrococcus* spp. and Gram-negative *Acinetobacter* spp., without the presence of pathogenic bacteria or overgrowth of any bacterial species. Details of signalment and microbiological culture are available in the Supporting Information (Table S1). Ten FFPE skin samples from dogs that had no history, clinical signs or histological evidence of skin disease were selected as controls. Control dogs were presented for surgery either for fracture repair, orchidectomy or ovariohysterectomy; skin samples were obtained from excess skin that was taken from surgical wound margins that are routinely taken for better wound apposition. Five samples were from dogs younger than 18 months, matching the juvenile onset demodicosis group and five samples were from dogs over 4 years of age, matching the adult-onset demodicosis group. The control samples were assessed histologically by author PAK (ECVP pathologist) for the presence of *Demodex* mites; all control samples showed no evidence of *Demodex* mites. Microbiological culture of the control skin samples was not carried out as the area from which these samples were taken had been cleaned and prepared for surgery. It is therefore presumed that culture would have yielded no growth. Also, the samples were assessed histologically and only those that showed no evidence of inflammation or skin disease were included. Details of signalment of the control cases are available in the Supporting Information (Table S1).

2.1.2 | Protein Extraction

Up to three scrolls from each FFPE block, with a thickness of up to 15 μm and a tissue area of up to 100 mm^2, were trimmed using a microtome and placed into sterile 2-mL collection tubes. Samples once cut were kept at −80°C until they could be deparaffinised. Deparaffinisation was carried out using heptane and methanol. Protein extraction from the deparaffinised sample was carried out using the Qiagen Qproteome kit (Qiagen, Hilden, Germany) as per the manufacturer's protocol. Briefly, following deparaffinisation, extraction buffer (EXB plus, Qiagen) supplemented with β-mercaptoethanol was added and the samples were heat treated. In preparation for MS, the protein was isolated using chloroform, methanol and ddH_2O separation. The protein samples were then dissolved in 1% (w/v) RapiGest (Waters Corp, Etten-Leur, the Netherlands) and were digested to peptides using a trypsin digest, as indicated in the Qproteome kit protocol.

2.1.3 | Mass Spectrometry

Following trypsin digestion, the peptides were cleaned using C18 ZipTip (Merck Millipore, Danvers, MA, USA). Samples were run on a Bruker timsTOF Pro mass spectrometer (Bruker Daltonics, Bremen, Germany) connected to an Evosep One system (EvoSep BioSystems, Odense, Denmark). Tryptic peptides were loaded onto Evotips and separated on a reversed-phase C18 Endurance column (15 cm × 150 μm ID, C18, 1.9 μm) using the pre-set 30

SPD method. Mobile phases were 0.1% (v/v) formic acid in ddH_2O (Phase A) and 0.1% (v/v) formic acid in acetonitrile (Phase B). The peptides were separated by an increasing gradient of mobile Phase B for 44 min using a flow rate of 0.5 μL/min.

The mass spectrometer was operated in positive ion mode with TIMS (trapped ion mobility spectrometry) and PASEF (parallel accumulation serial fragmentation) enabled. The accumulation and ramp times for the TIMS were both set to 100 ms, with an ion mobility (1/*k*0) range from 0.6 to 1.6 Vs/cm. A scan range of 100–1700 *m*/*z* was performed at a rate of 10 PASEF MS/MS frames to 1 MS scan with a cycle time of 1.17 s.

2.1.4 | Proteomic Data Analysis

Protein identification and label-free quantification (LFQ) normalisation of MS/MS data was performed using MaxQuant v2.0.3.0 (www.maxquant.org) [30]. Variable modifications selected were acetyl (protein N-term) and oxidation (M), while trypsin was selected as the digestion enzyme and the maximum number of allowed missed cleavage was two. MS/MS data were correlated against the *Canis lupus familaris* reference proteome downloaded from Uniprot (January 2023) using the Andromeda search algorithm incorporated in MaxQuant software, including a contaminant sequence set. Data analysis, processing and visualisation were performed using Perseus v.2.1.4.0 (www.maxquant.org) following standard steps for LFQ analysis [31]. Briefly, LFQ-normalised peptide-intensity values from the MaxQuant analysis were used to quantify protein abundance. Data were filtered to remove protein groups that were identified only by peptides that carry one or more modified amino acids, those matching to the reverse database and those identified as potential contaminants. Then $\log_2$ transformation was performed, with subsequent grouping of samples according to aetiology (control, demodicosis). Further filtering was performed whereby only proteins present in at least 70% of samples were retained, and a two-sample *t*-test was performed. Statistical testing was done at the two-tailed α level of 0.05 ($p < 0.05$) to identify significantly differentially abundant proteins across the two aetiologies. In addition, we also used the permutation-based *q* false discovery rate (FDR) method to adjust *p* values and correct for multiple testing [32, 33]. A *q* value threshold of 0.01 was used to further filter differentially abundant proteins. The MS proteomics data have been deposited to the ProteomeXchange Consortium via the PRIDE partner repository with the data set identifier PXD050219 [34].

2.1.5 | Metascape Analysis

Metascape is an online software based on the OMICS database [35]. It has functions such as functional enrichment, interactome analysis, gene annotation and membership search, and it can analyse and annotate given genes. The Metascape (v3.5.20230501) express analysis function was used to analyse the functions and pathways of the protein groups identified as either in significantly high abundance or in low abundance. The *q* FDR (0.01) method was applied to filter the input gene symbols. Only protein groups in which gene symbol IDs were available were used for the gene ontology (GO) overrepresentation analyses (ORAs). The set of background genes used were the gene IDs of proteins found across both the demodicosis and control groups.

2.1.6 | Ingenuity Pathway Analysis

Ingenuity Pathway Analysis (IPA) software [36] was used with the Ingenuity Knowledge Base (Qiagen, Redwood City, CA, USA; release date December 2022) to identify enriched canonical pathways for the differentially abundant proteins that had corresponding gene symbols. IPA Core Analysis was performed using the default settings with the user data set as the background, high predicted confidence and all nodes selected. As with the Metascape analysis, *q* FDR (0.01) method was applied to filter the input gene symbols. For the identification of overrepresented canonical pathways, a stringent Benjamini–Hochberg (B–H) *p*-value adjustment was also applied with a B–H FDR p_{adj} threshold <0.05 [37].

2.2 | Immunohistochemistry

2.2.1 | Case Selection

Ten FFPE skin samples from dogs diagnosed histologically with canine demodicosis were selected.

These samples had no microbiological culture carried out; however, the samples were assessed histologically to ensure there was no overt evidence of bacterial skin disease by the author PAK (ECVP pathologist). A further 10 FFPE skin samples from dogs that had no history, gross or histological evidence of skin disease were selected as controls. Details of signalment of cases are available in the Supporting Information (Table S2).

2.2.2 | Immunohistochemistry

The antibodies applied are common cell markers used to identify different lineages of macrophage and dendritic cells in tissues. Detailed methods for immunohistochemistry are available in the Supporting Information S1. Briefly, 5-μm thick sections were prepared from the FFPE tissue blocks for each case, rehydrated and stained by immunoperoxidase methods indicated in Table 1. 3,3′-Diaminobenzidine (DAB) was used as the chromogen and Gill's haematoxylin as counterstain.

TABLE 1 | Antibodies and immunohistochemical procedures.

Antibody	Dilution	Incubation (min)	Pre-treatment	Source
IBA-1	1:1500	30	HIER, citrate buffer, pH 6	Wako Chemical
CD301	1:50	30	HIER, citrate buffer, pH 6	Invitrogen
CD90	1:100	60	Proteinase K	Novus Biologicals
CD163	1:250	30	DIVA	Novus Biologicals
E-cadherin	1:200	30	DIVA	Cell Signaling Technology
CD204	1:100	30	Proteinase K	Novus Biologicals

2.2.3 | Evaluation of Immunostaining

Using an Olympus BX41 microscope (Olympus Optical Co., Tokyo, Japan) connected to a digital camera (SC50, Olympus), five representative areas were selected that showed the highest population of positive immunolabelled cells within each tissue section. These were imaged using the 400× power objective and saved as JPEG files. To allow for comparison of immunolabelling across multiple skin samples, image acquisition was performed in parallel for the entire set, using identical settings and exposure times. The image analysis software ImageJ (version 1.54d) was used to quantify the expression of each marker using the IHC profiler plugin [38, 39]. This IHC analysis tool uses colour deconvolution and computerised pixel profiling, leading to the assignment of automated scores to the respective image of % high positive, % positive, % low positive and % negative stained cells. The high-positive, positive and low-positive scores were combined to provide a total percentage score of immunolabelled positive cells within an image. This percentage of total positive scores was used for statistical analysis. Student's *t*-test was used to compare the means between the demodicosis group and the control group ($p < 0.05$).

3 | Results

3.1 | Proteome Profile

The general proteome profiling of the analysed skin samples was examined to identify differences in protein group paucity or abundance. We identified 1123 protein groups across all samples (Table S3), after removing proteins identified by site, matching to the reverse database and contaminants. Following further filtering for at least 70% of valid values (i.e., removing protein groups with <70% valid values), a total of 942 protein groups were found across the samples. Principal component analysis (PCA) was performed based on the protein abundance values from LC–MS/MS. A plot of the first two principal components (PC1 and PC2) (Figure 1) showed clear differentiation and clustering of samples within the canine demodicosis ($n = 10$) and control ($n = 10$) groups, and with 24.5% and 12.5% of the variation explained by PC1 and PC2, respectively. Filtering by the FDR-adjusted *p*-value ($q < 0.01$) showed that 267 protein groups were significantly differentially expressed between the two groups (Figure 2 and Table S4). Of these protein groups, 154 were observed to be more highly and 113 more lowly abundant, respectively, in the demodicosis group compared with the control group. The 20 most abundant and 20 least abundant proteins for this contrast are detailed in Tables 2 and 3.

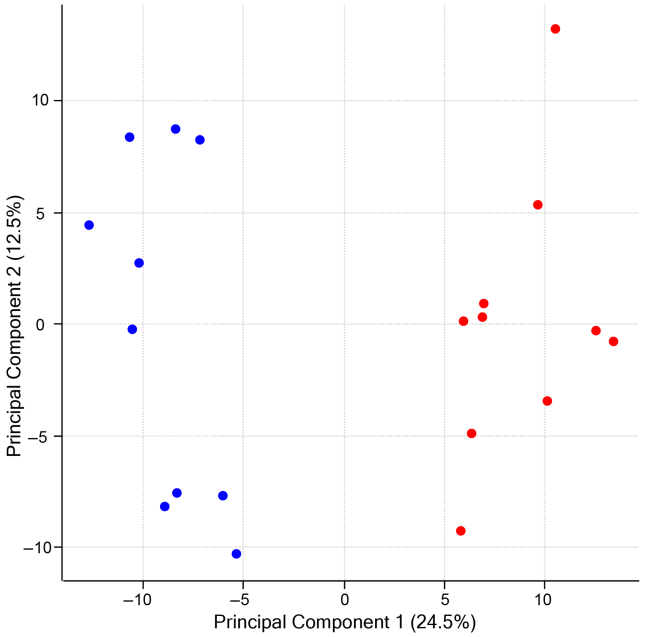

FIGURE 1 | Principal component analysis (PCA). Each data point represents a sample with control samples shown in blue and demodicosis samples shown in red.

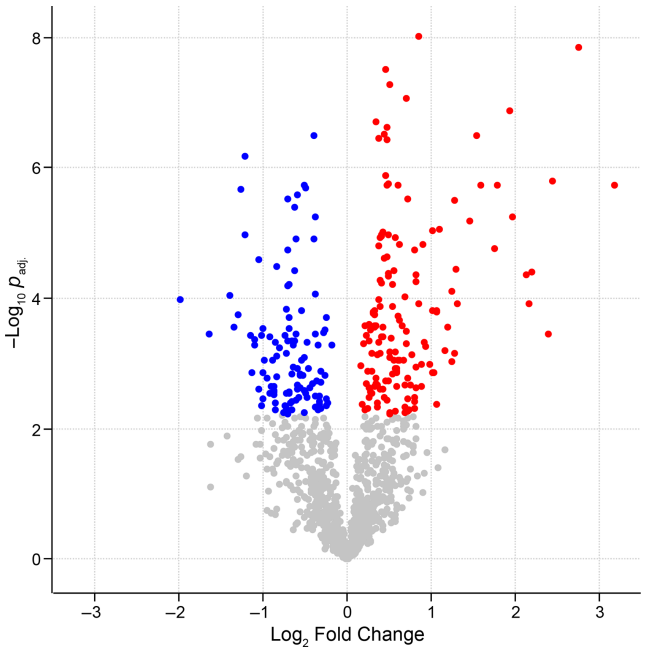

FIGURE 2 | Volcano plot of proteins found to be significantly differentially abundant in the demodicosis group compared with the control group ($q < 0.01$). Proteins with significantly decreased abundance are shown in blue and proteins with significantly increased abundance are shown in red.

3.2 | Pathway Analysis

Results from the Metascape GO ORA of 131 highly and 110 lowly abundant proteins (with available gene symbol IDs) are shown in Figure 3. The analysis used the proteins observed across all samples (1123 proteins, with 1020 gene symbol IDs available) as the background set for the ORA.

From the set of 1123 detectable protein groups found across all samples, 1080 had corresponding gene symbol IDs and 1015 of these could be mapped within IPA. The majority of those unmapped (55/65) were LOC gene symbols, for which a formal ID has not yet been determined. The B–H FDR $p_{adj.}$ (q) threshold <0.01 gave 238 gene symbol IDs for the IPA analysis, 132 of which had an increased $\log_2$ fold change ($\log_2$FC) and 106 of which had a decreased $\log_2$FC against a background data set of 1014 analysis-ready gene symbols, 507 of which had an increased $\log_2$FC and 507 of which had a decreased $\log_2$FC. With a B–H FDR $p_{adj.}$ threshold <0.05, there were four statistically

TABLE 2 | The 20 most statistically significant proteins displaying increased abundance of the demodicosis case group compared with the control group ($q < 0.01$).

Protein name	Gene	Location	*q* (adjusted *p*) value
Myeloperoxidase	*MPO*	Cytoplasm	0.00001
Protein S100A12	*S100A12*	Cytoplasm	0.00001
Cornifin like	*LOC119868937*	Cytoplasm	0.00001
EF-hand domain-containing protein	*S100A9*	Cytoplasm	0.00001
Coronin	*CORO1A*	Cytoplasm	0.00001
Major histocompatibility complex, Class II, DQ alpha 1	*DLA-DQA1*	Plasma membrane	0.00001
Cathepsin C	*CTSC*	Cytoplasm	0.00001
Cathepsin S	*CTSS*	Cytoplasm	0.00001
Glia maturation factor	*GMFG*	Cytoplasm	0.00001
Ras homolog family member	*RHOG*	Cytoplasm	0.00001
Lymphocyte cytosolic protein 1	*LCP1*	Cytoplasm	0.00001
Profilin	*PFN1*	Cytoplasm	0.00001
PYD and CARD domain-containing protein	*PYCARD*	Cytoplasm	0.00001
Actin-related protein 3 O	*ACTR3*	Plasma membrane	0.00001
Actin-related protein 2/3 complex subunit 4	*ARPC4*	Cytoplasm	0.00001
60S acidic ribosomal protein P2	*RPLP2*	Cytoplasm	0.00001
40S ribosomal protein SA	*RPSA*	Cytoplasm	0.00001
B-cell antigen receptor complex-associated protein alpha chain	*CD79A*	Plasma membrane	0.00001
60S ribosomal protein L9	*RPL9*	Nucleus	0.00001
Enolase 1	*ENO1*	Cytoplasm	0.00001
Chloride intracellular channel protein	*CLIC1*	Nucleus	0.00001
60S acidic ribosomal protein P0	*LOC481399*	Cytoplasm	0.00001
40S ribosomal protein S8	*RPS8*	Cytoplasm	0.00001
Phosphoglycerate mutase	*PGAM1*	Cytoplasm	0.00001
Serine/arginine-rich splicing factor 1	*SRSF1*	Nucleus	0.0001

significant enriched IPA canonical pathways: *eIF2 Signalling*, *Coronavirus Pathogenesis Pathway*, *mechanistic target of rapamycin* (*mTOR*) *Signalling* and *Regulation of eIF4 and p70S6K Signalling* (Figure 4). A schematic diagram of each of these pathways highlighting the differentially expressed molecules is provided in Figures S1–S4.

Ten statistically significant upstream regulators were identified by IPA (Table S5). The top activated upstream regulators were 3,5-dihydroxyphenylglycine and MLXIPL. The inhibited upstream regulators included FMR1 and LARP1. The top three ranked IPA diseases and disorders are shown in Figure 5 consisting of *Immunological Disease*, *Organismal Injury and Abnormalities*, and *Inflammatory Response*.

3.3 | Immunohistochemistry

Antibodies against common monocyte, dendritic cell and macrophage markers consisting of IBA-1, E-cadherin, CD163, CD301, CD90 and CD204 were applied to FFPE skin samples from 10 dogs with canine demodicosis and 10 dogs with no history or histological evidence of skin disease (control group). All cases of canine demodicosis had significantly higher numbers of cells expressing positive immunolabelling for all antibodies ($p \leq 0.01$), except for CD204 ($p > 0.05$), compared with the control group (Figures 6 and 7).

4 | Discussion

The objective of this study was to assess the proteomic profiles of FFPE skin samples from dogs with canine demodicosis and compare these profiles with those from healthy canine controls. The aim was to provide further molecular insights into the pathogenesis of canine demodicosis. We identified 1123 protein groups across all samples, which is in keeping with the number of proteins identified from FFPE tissues in other studies [40, 41]. Our study showed 154 protein groups to be significantly more highly abundant and 113 more lowly abundant in the demodicosis group compared with the control group. To further investigate these data, we employed two functional omics data analysis software tools, Metascape and IPA, which can be used to identify biologically relevant signalling and metabolic pathways, reconstruct molecular networks, predict the direction of downstream effects on biological and disease processes, and predict the activation and inhibition of upstream regulators [35, 36].

TABLE 3 | The 20 most statistically significant proteins displaying decreased abundance of the demodicosis case group compared with the control group ($q < 0.01$).

Protein name	Gene	Location	*q* (adjusted *p*) value
Acyl-CoA dehydrogenase very long-chain O	*ACADVL*	Cytoplasm	0.00001
Actinin alpha 1	*ACTN1*	Cytoplasm	0.00001
Basal cell adhesion molecule	*BCAM*	Plasma membrane	0.0001
Caveolae associated protein 1	*CAVIN1*	Nucleus	0.00018
Carboxylesterase 5A	*CES5A*	Extracellular space	0.00073
EH domain-containing protein 2	*EHD2*	Nucleus	0.000082
Fetuin B	*FETUB*	Extracellular space	0.00072
Four and a half LIM domains 1	*FHL1*	Cytoplasm	0.000451
Filamin C	*FLNC*	Cytoplasm	0.000438
Guanine deaminase	*GDA*	Cytoplasm	0.000585
Glutathione S-transferase mu 3	*GSTM3*	Cytoplasm	0.00001
Isocitrate dehydrogenase (NADP)	*IDH1*	Cytoplasm	0.000091
Keratin 4	*KRT77*	Cytoplasm	0.000636
IF rod domain-containing protein	*KRT86*	Cytoplasm	0.000108
Laminin subunit beta 2	*LAMB2*	Extracellular space	0.000093
Laminin subunit gamma 1	*LAMC1*	Extracellular space	0.00001
ATP synthase subunit b	*LOC119872230*	Mitochondria	0.00001
Malate dehydrogenase	*MDH1*	Cytoplasm	0.000343
Myosin heavy chain 14	*MYH14*	Extracellular space	0.000176
Nidogen 1	*NID1*	Extracellular space	0.00001
Podocan	*PODN*	Cytoplasm	0.0000076
Pre-mRNA processing factor 8	*PRPF8*	Nucleus	0.0006
Transmembrane protein 43	*TMEM43*	Nucleus	0.00001
Tropomyosin 1	*TPM1*	Cytoplasm	0.000143
Vinculin	*VCL*	Plasma membrane	0.00001

Metascape analysis was used with both the high and low abundant proteins. Metascape uses an ORA method to assess the enrichment of pathways in a gene list compared with a background comparator list. It does not rank/prioritise proteins/genes based on statistical significance or differential expression (i.e., $\log_2$FC or $p_{adj.}$ value). Among the enriched ontology clusters in our study, we identified the *PI3 AKT pathway*. Although commonly associated with neoplasia, this pathway also plays a critical role in inflammation. It regulates Toll-like receptor (TLR) activity and NF-kB signalling in macrophages, leading to their polarisation into M2 immunosuppressive macrophages [42, 43]. The presence of *Antigen Processing and Presentation of Exogenous Antigen Pathway* is not surprising given the presence of the exogenous *Demodex* mites. Similarly, the presence of *TNF Pathway*, *Leukocyte Activation* and *Leukocyte Cell–Cell Adhesion* is expected given the presence of inflammatory cells within the tissues assessed. The *TNF pathway* is essential for the immediate immune response and is involved in the innate immune system through cell activation, proliferation, apoptosis and necrosis [44].

IPA was used for gene set enrichment analysis (GSEA) in which proteins/genes can be ranked by statistical significance or expression difference (i.e., $p_{adj.}$ or $\log_2$FC), and statistically analysed for enrichment of specific pathways or other functional biological categories using detectable proteins/genes as the background comparator set. All gene symbol IDs for the significantly differentially abundant proteins were used for the IPA analysis. This analysis identified four statistically enriched canonical pathways for canine demodicosis with biological processes and molecular functions similar to those identified by Metascape. One of these pathways, the *Coronavirus Pathogenesis Pathway*, was incorporated into the Ingenuity Knowledge Base in recent years [45] and has been observed in other studies of non-coronavirus infectious diseases [46]. The three other significantly enriched signalling pathways, *eIF2 Signalling*, *mTOR Signalling* and *Regulation of eIF4 and p70S6K Signalling*, are involved in regulation of initiation of transcription and translation in response to a range of stress stimuli, both external and internal [47–49]. These pathways have also been shown to be inextricably linked [16, 49] and all have been shown to be involved in the modulation of TLRs [50, 51]. Moreover, these pathways have been previously demonstrated to play a role in the pathogenesis of skin diseases such as rosacea, psoriasis, atopic dermatitis and melanoma in both dogs and humans [52–56].

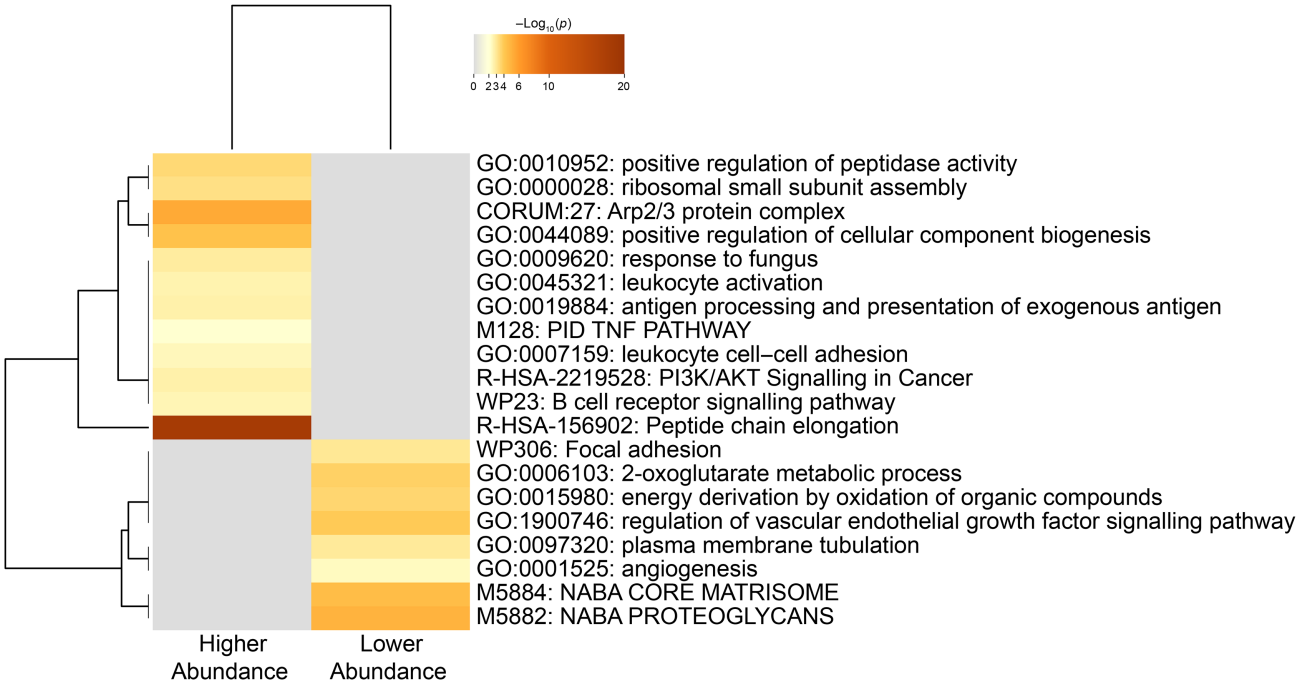

FIGURE 3 | Heatmap showing the enrichment ontology clusters obtained by Metascape enrichment analysis from the most significant high abundance and low abundance proteins found in the canine demodicosis group compared with the control group.

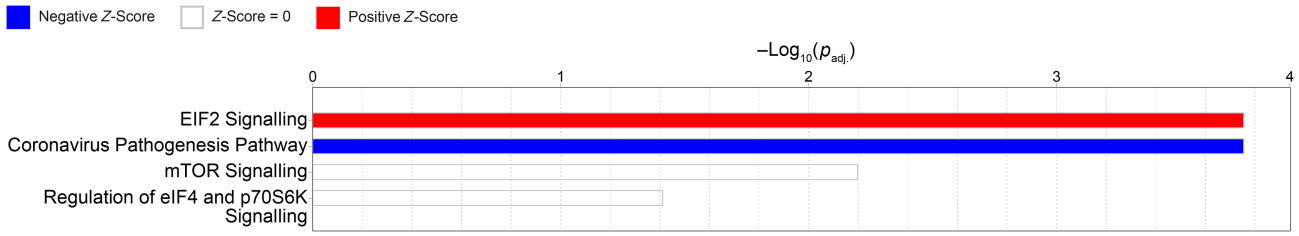

FIGURE 4 | Bar chart showing the four statistically significant enriched IPA canonical pathways in order of decreasing $-\text{Log}_{10}$ ($p_{\text{adj.}}$): *EIF2 signalling*, *Coronavirus pathogenesis pathway*, *mTOR signalling*, and *regulation of eIF4 and p70S6K signalling*. The red and blue colours of the bars indicate the predicted pathway activation or inhibition, respectively. White bars indicate pathways for which the *Z*-score is zero.

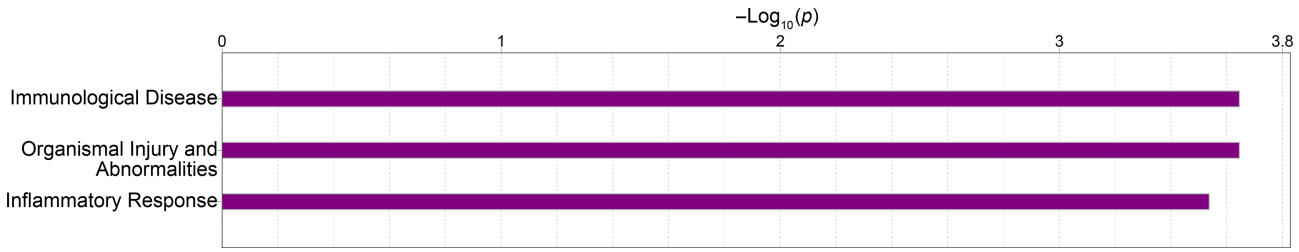

FIGURE 5 | Bar chart showing the top three diseases, disorders and biological functions identified using IPA.

Cell stress, whether from internal or external sources, can cause improper protein folding, resulting in the accumulation of misfolded or unfolded proteins in the endoplasmic reticulum (ER), known as ER stress. To combat this, unfolded protein response (UPR) is initiated to restore normal ER function and reduce ER stress [54]. The UPR reduces protein translation, increases degradation of misfolded/unfolded proteins and increases the expression of ER chaperones and folding enzymes to improve protein folding. The eukaryotic translation initiation factor 2 (eIF2) signalling pathway is involved in the UPR, which regulates protein synthesis initiation. When eIF2 is phosphorylated, it inhibits eIF2B activity, leading to reduced protein synthesis and reduced protein-folding load in ER-stressed cells. eIF2α selectively induces translation of activating transcription factor 4 (ATF4), which controls expression of adaptive genes that protect cells against ER stress. ER stress, through activation of ATF4, has been shown to affect pro-inflammatory cytokine production by modulating TLR signalling, mostly notably through TLR2 [50]. ER stress via ATF4 also increases VEGF-A expression, stimulating

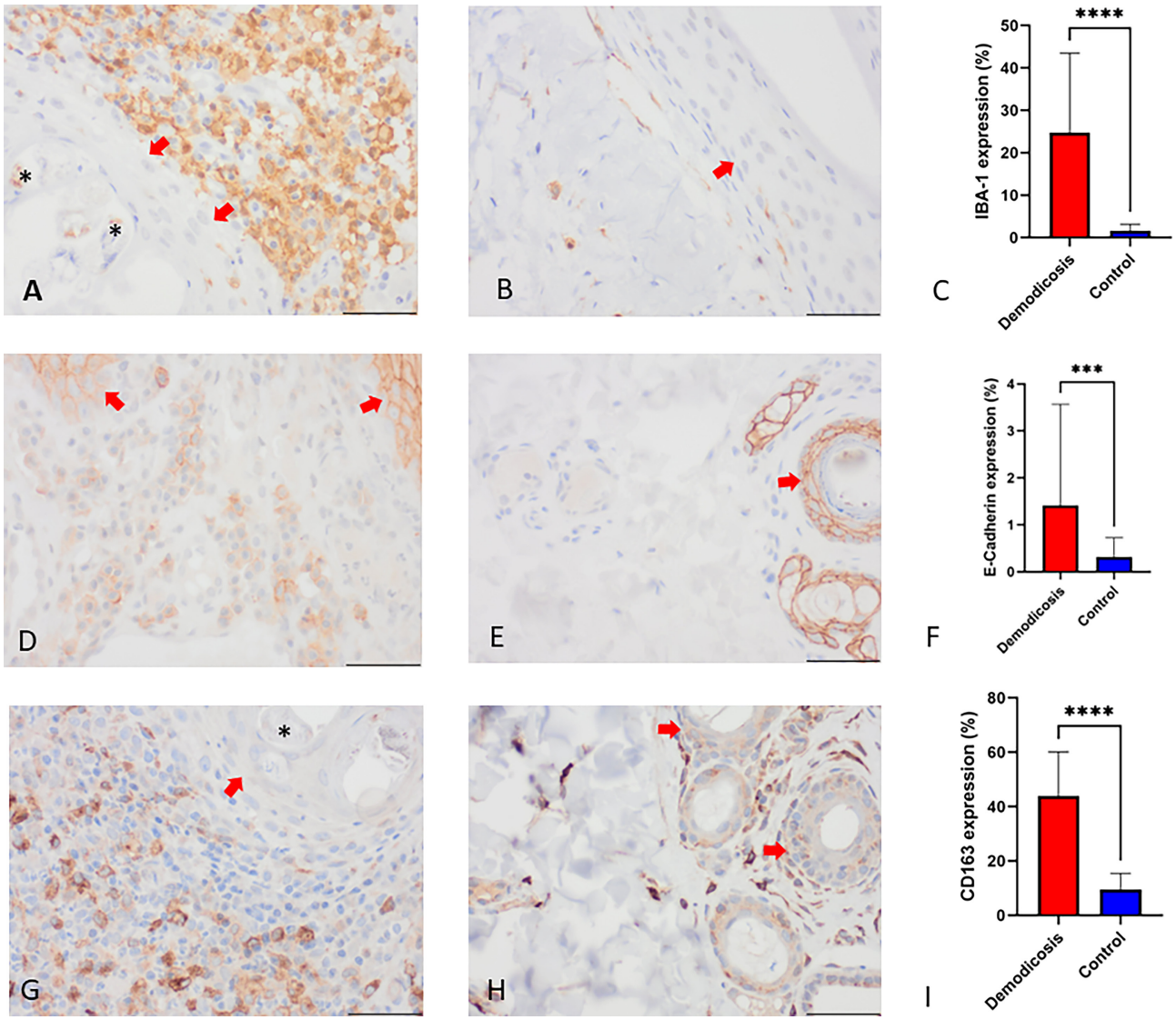

FIGURE 6 | (A) Skin from a canine demodicosis case, innumerable IBA1-positive immunolabelled cells are adjacent to a hair follicle (red arrow) containing a *Demodex* mite (*). (B) Control skin, scattered IBA-1-positive immunolabelled cells within the dermis and extending into the outroot sheet of the hair follicle (red arrow). (C) Bar chart of percentage IBA-1-positive immunolabelled cells in cases of demodicosis in comparison with controls (****$p < 0.0001$). (D) Skin from a canine demodicosis case, moderate numbers of E-cadherin-positive immunolabelled cells are adjacent to two hair follicles (red arrow) that show normal E-cadherin expression. (E) Control skin, hair follicle epithelium (red arrow) is positively immunolabelled with E-cadherin (normal expression). (F) Bar chart of percentage of E-cadherin-positive immunolabelled cells within the dermis in cases of demodicosis in comparison with controls (***$p < 0.001$). (G) Skin from a canine demodicosis case, numerous CD163-positive immunolabelled cells are adjacent to a hair follicle (red arrow) containing a *Demodex* mite (*). (H) Control skin, scattered CD163-positive immunolabelled cells are present within the dermis. Red arrow indicates hair follicles. (I) Bar chart of percentage of CD163-positive immunolabelled cells in cases of demodicosis in comparison with controls (****$p < 0.0001$).

angiogenesis and inflammatory lymphangiogenesis, which play a significant role in chronic skin inflammation [57]. Both TLR2 and VEGFA have been shown previously to be upregulated in lesional skin from dogs with demodicosis [13, 58]. The findings suggest that ER stress–induced UPR signalling through the eIF2 pathway may contribute to the pathogenesis of canine demodicosis by upregulating TLR2 and activating the VEGFA–VEGFR2 signalling pathway.

There is growing evidence that the ER stress and UPR response are modulators of immunity [59]. Recent work has demonstrated that the ER stress and the UPR response are involved in regulating multiple immune cell types including T cells, B cells, DCs, macrophages and myeloid-derived suppressor cells (MDSCs) [59–62]. More specifically, ER stress and UPR responses have been shown to regulate differentiation, cytokine production, exhaustion and apoptosis of CD8+ T cells as well as induce regulatory T-cell plasticity. Additionally, the responses have been shown to support the survival of immunosuppressive MDSCs, trigger these cells to produce immunosuppressive iNOS, ROS and Arg-1, promote IL-10 secretion and promote an immunosuppressive M2 macrophage phenotype [63–66].

In our previous gene expression study, we observed an increase in regulatory T cells and detected a gene expression pattern

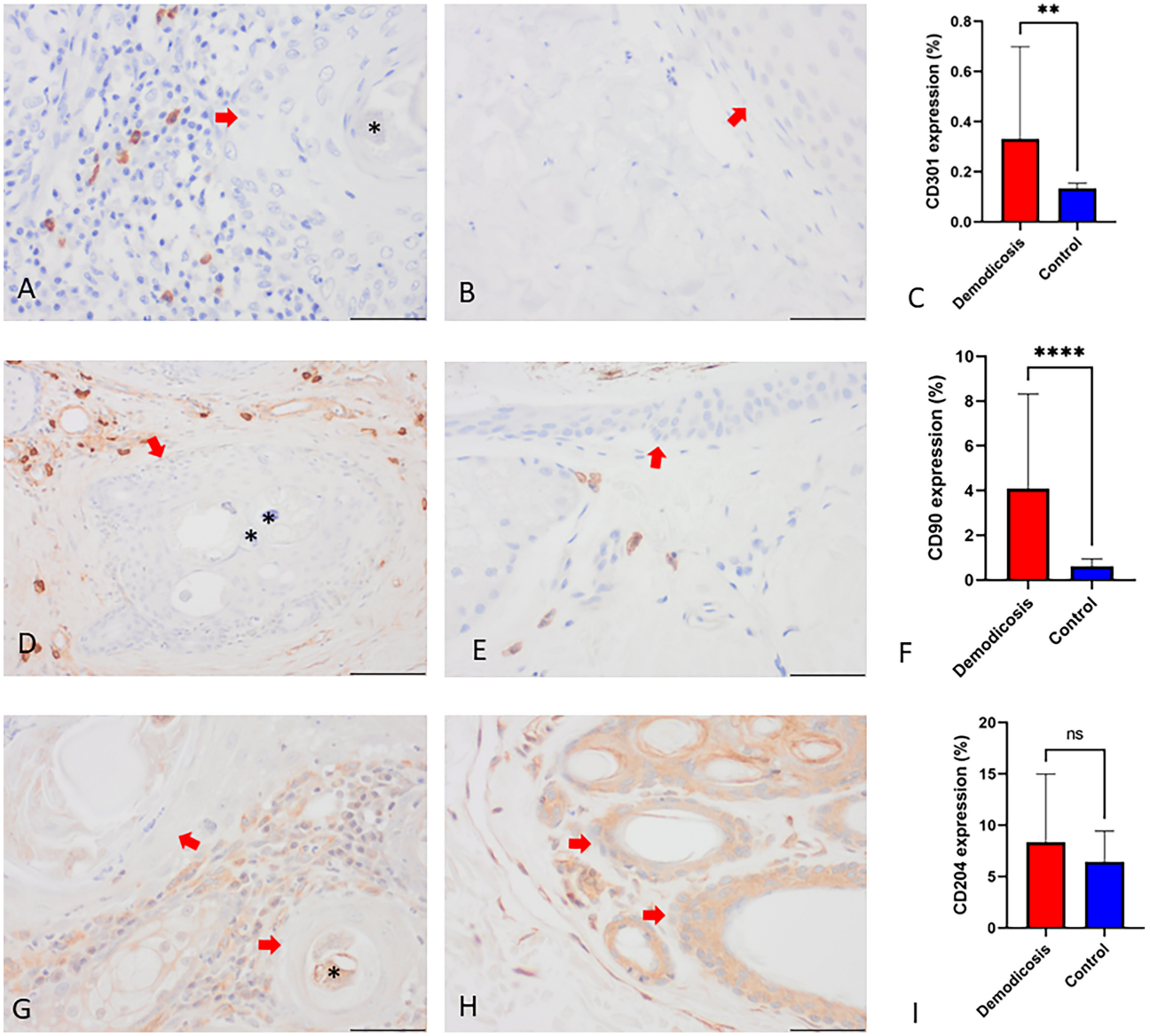

FIGURE 7 | (A) Skin from a canine demodicosis case, scattered CD301-positive immunolabelled cells are adjacent to a hair follicle (red arrow) containing a *Demodex* mite (*). (B) Control skin, the dermis and hair follicle (red arrow) show no CD301 immunolabelled cells. (C) Bar chart of percentage of CD301-positive immunolabelled cells in cases of demodicosis in comparison with controls (**$p < 0.01$). (D) Skin from a canine demodicosis case, moderate numbers of CD90-positive immunolabelled cells surround a hair follicle (red arrow) that contains *Demodex* mites (*). (E) Control skin, scattered CD90-positive immunolabelled cells are seen in the perifollicular areas. Hair follicle indicated by a red arrow. (F) Bar chart of percentage of CD90-positive immunolabelled cells within the dermis in cases of demodicosis in comparison with controls (***$p < 0.00001$). (G) Skin from a canine demodicosis case, numerous CD204-positive immunolabelled cells are adjacent to hair follicles (red arrows). *Demodex* mites (*) are present in hair follicles. (H) Control skin, scattered CD204-positive immunolabelled cells are present within the dermis surrounding hair follicles (red arrow), which also display non-specific cytoplasmic immunolabelling. (I) Bar chart of percentage of CD204-positive immunolabelled cells in cases of demodicosis in comparison with controls (ns, $p > 0.05$).

indicative of the presence of immunosuppressive MDSCs and M2 macrophages in cases of canine demodicosis [58]. Based on the pathways highlighted in both the Metascape and IPA analyses, specifically the PI3 AKT pathway and eIF2 signalling pathway, which are associated with the polarisation of macrophages towards the M2 phenotype, we investigated the presence of M2 macrophages in lesional skin from dogs with demodicosis. To accomplish this, we employed immunohistochemical markers commonly used for identifying dendritic cells and macrophages on the FFPE tissue. In canine demodicosis, we observed a marked infiltration of cells positively immunolabelled with IBA-1, indicating the proliferation of Langerhans cells (LC), interstitial dendritic cells and macrophages. Furthermore, we observed a significant infiltration of E-cadherin-positive (cytoplasmic and membranous) immunolabelled cells in the dermis, which confirm an increase in LCs and their mobilisation from the epidermis to the dermis. Research in the field of *Leishmania*, a protozoan parasite, has shown that LCs cause an increase IL-10 and regulatory T cells [67]. It is therefore possible that LCs are playing a role in promoting an immunosuppressive environment in canine demodicosis through similar pathways of IL10 production and induction of regulatory T cells. We also found

an increase in CD90-positive cells in the demodicosis group, indicating proliferation of interstitial dendritic cells. Additionally, we observed a significant increase in CD163- and CD301-positive immunolabelled cells, which are common markers for M2 macrophages in the demodicosis group [68–71]. M2 macrophages are known to produce immunosuppressive cytokines IL-10 and TGF-β together with growth factor VEGF [72]. The immunohistochemical findings of significant infiltrations of CD163- and CD301-positive immunolabelled cells confirm the presence of M2 macrophages and support their role in creating the immunosuppressive microenvironment seen in canine demodicosis.

The presence of M2 phenotype macrophages, along with the proteomic evidence of upregulated UPR response through *eIF2 signalling* pathway, supports the hypothesis that *Demodex* mites induce ER stress, resulting in the modulation of immunity towards an immunosuppressive, immune-tolerant phenotype. Additionally, our previous findings of increased T-regulatory cells and a gene expression profile supporting the presence of MDSC further reinforce this hypothesis; however, further research into the canine MDSCs is required [58]. Similar research into other pathogens, mostly protozoan infections and mycobacterial diseases, support the ability of microorganisms to induce ER stress, utilise the UPR response and polarise macrophages to the M2 immunosuppressive phenotype to avoid immune detection and allow for their proliferation [73, 74].

The protein known as mTOR plays a crucial role in the growth, proliferation and differentiation of keratinocytes [75]. mTOR is part of the PI3K/Akt signalling pathway, which, as noted earlier, plays a crucial role in regulation of inflammation. Previous studies investigating the role of mTOR signalling in helminth infections have shown that the pathway promotes M2 macrophage differentiation [71]. This suggests the possibility of a role for mTOR signalling in regulating the M2 macrophages seen here in canine demodicosis. Disruption or dysregulation of mTOR can also affect protein synthesis and thereby impact cell growth and proliferation, leading to various skin diseases [76]. Inflammatory cytokines such as IL-22, IL-17 and TNF can induce hyperactivation of the mTOR pathway, resulting in enhanced keratinocyte proliferation and reduced differentiation, as observed in the human skin disease, psoriasis [52]. A common histological change in canine demodicosis is epidermal and follicular epithelial hyperplasia; it could be postulated, given the current study, that this change is influenced by mTOR hyperactivation [4, 77]. mTOR has also been implicated in the pathogenesis of rosacea, a human skin disease that is often compared with canine demodicosis due to increased populations of *Demodex* mites in lesional skin [78]. Cathelicidin, LL-37, an antimicrobial peptide, which is increased in the skin of rosacea patients, activates the mTOR pathway by binding TLR2 and results in increased expression of cathelicidin itself in keratinocytes. Also, it has been shown that cathelicidin again through mTOR signalling induces NF-kB activation, resulting in cytokines and chemokines characteristic of rosacea, and topical application of rapamycin, an mTOR inhibitor, results in improved clinical signs [78]. Upregulation of TLR2 has also been shown in canine demodicosis, which may result in activation of the mTOR pathway, thereby contributing to the cytokines and chemokines produced. mTOR has also been shown to be involved in angiogenesis in rosacea patients through increased cathelicidin and increased VEGF expression [79]. While VEGFA expression has been shown to be increased in canine demodicosis, its role in disease development and progression has not yet been elucidated [58].

The eIF4 and p70S6K signalling pathway is positively regulated by mTOR and constitutes the main pathway for cell proliferation, survival, differentiation and angiogenesis. Various stimuli, such as growth factors and cytokines, activate this pathway by triggering a phosphorylation cascade involving PI3K, Akt, PDK1 and mTOR [49]. Activation of the PI3K/Akt/mTOR/p70S6K pathway impacts angiogenesis by the upregulation of VEGF [80]. Dysregulation of this pathway was observed in the current study; however, its role and the role of VEGF in canine demodicosis remain to be clarified.

IPA enrichment analysis identified immunological disease, organismal injury and abnormalities, and inflammatory response as the most significant underlying diseases and disorders. This is consistent with what would be expected for an inflammatory disease due to an ectoparasite. Reflecting the inflammatory nature of canine demodicosis, genes of several inflammatory proteins found in abundance in the current study were also found to be differentially expressed in a recent transcriptome study of canine atopic dermatitis (CAD) by Tengvall et al. [81]. Among the significantly differentially expressed genes identified, *S100A12*, *S100A9*, *DLA79* and *DLA-12* were found in the untreated CAD compared with control skin samples from healthy canines [81]. Interestingly, these genes were also observed to be abundant in the current proteomic study on demodicosis. S100A12, known as a pro-inflammatory protein secreted by neutrophils, and S100A9, an alarmin protein capable of upregulating pro-inflammatory cytokines, were among the proteins identified [82]. Additionally, dog leukocyte antigen (DLA), a component of the major histocompatibility complex (MHC) in dogs, which encodes genes within the MHC, was also implicated. Given the commonality of investigating inflammatory skin diseases in both studies, the presence of similar findings is not unexpected. This supports the correlation between transcriptomic and proteomic profiles in canine dermatological conditions, highlighting the interplay between gene expression and protein abundance in disease.

This study has some limitations, such as the small number of significantly different protein groups (267) found between the disease and control groups. However, it is the first proteomic profiling study of skin samples from dogs with canine demodicosis. The skin samples used in this study were FFPE. Although formalin fixation causes significant cross-linking among proteins and other biomolecules, several studies have shown that there is a significant overlap in the number and identities of proteins between FFPE and frozen tissue [83–85]. This indicates that there is an equivalence in proteomic profile obtained from fresh-frozen and FFPE tissue specimens by shotgun proteomics. Another limitation of this study is the utilisation of distinct cohorts for the proteomic and immunohistochemical investigations, which was necessitated by the availability of small tissue samples alone from clinical cases. The limited amount of available tissue is a persistent constraint in research endeavours. However, although this aspect can be perceived as a limitation, it also serves as a strength, as it not only demonstrates a proteomic profile indicative of M2 macrophages in 10 cases but also confirms the presence of cells exhibiting M2 macrophage markers in an additional 10 cases.

5 | Conclusion

The aim of this study was to gain molecular insights into the pathogenesis of canine demodicosis by employing proteomics and pathway enrichment analysis. Our findings revealed significant dysregulation in several interconnected pathways that regulate transcription and translation initiation in response to various internal and external stress stimuli. Furthermore, our pathway enrichment analysis using the proteomic profile identified immunological disease, organismal injury and abnormalities and inflammatory response as the most significantly associated diseases and disorders. Immunohistochemistry confirmed the presence of M2 macrophages in lesional skin from dogs with demodicosis. Overall, our study suggests that *Demodex* mites trigger ER stress, inducing an UPR response, leading to the proliferation of M2 macrophages, which, in turn, contributes to an immunosuppressive microenvironment, promoting *Demodex* survival and proliferation.

Author Contributions

Pamela A. Kelly, Rory Breathnach: Funding acquisition. Pamela A. Kelly, Rory Breathnach: Conceptualization. Pamela A. Kelly: Investigation; Writing – original draft. Pamela A. Kelly, Caitriona Scaife, Gillian P. McHugo, Susan Peters: Data curation. Pamela A. Kelly, Caitriona Scaife, Gillian P. McHugo: Formal analysis. Pamela A. Kelly, Caitriona Scaife, Gillian P. McHugo, David E. MacHugh, Susan Peters, Marion Stevenson: Methodology; Validation. Pamela A. Kelly, Gillian P. McHugo, Caitriona Scaife, Susan Peters, Marion Stevenson, Jennifer S. McKay, David E. MacHugh, Irene Lara-Saez, Rory Breathnach: Writing – review and editing.

Acknowledgements

The authors acknowledge the assistance of the Purdue University Histology Research Laboratory, a core facility of the NIH-funded Indiana Clinical and Translational Science Institute, specifically laboratory manager Ms MacKenzie McIntosh, for the optimisation and staining of sections for E-cadherin, CD163, CD90 and CD204. We also thank Dr Jamie Timmons (Augur Precision Medicine) and Dr Mark Ziemann (Deakin University) for valuable advice concerning the functional omics data analyses. Open access funding provided by IReL.

Conflicts of Interest

The authors declare no conflicts of interest.

Data Availability Statement

The data that support the findings of this study are openly available in PRIDE at https://www.ebi.ac.uk/pride/, reference number Project accession: PXD050219.

Peer Review

The peer review history for this article is available at https://www.webofscience.com/api/gateway/wos/peer-review/10.1111/pim.13033.

References

1. R. S. Mueller, E. Bensignor, L. Ferrer, et al., "Treatment of Demodicosis in Dogs: 2011 Clinical Practice Guidelines," *Veterinary Dermatology* 23 (2012): 86–96 e20-1.

2. R. S. Mueller, W. Rosenkrantz, E. Bensignor, J. Karaś-Tęcza, T. Paterson, and M. A. Shipstone, "Diagnosis and Treatment of Demodicosis in Dogs and Cats," *Veterinary Dermatology* 31 (2020): 4-e2.

3. R. Foley, P. Kelly, S. Gatault, and F. Powell, "*Demodex*: A Skin Resident in Man and His Best Friend," *Journal of the European Academy of Dermatology and Venereology* 35 (2021): 62–72.

4. F. S. Valéria Régia, D. G. Naiani, and B. P. F. A. Arleana, "Chapter 4: Clinical and Immuno-Pathology Aspects of Canine Demodicosis," in *Parasitology and Microbiology Research*, eds. G. Antonio Bastidas Pacheco and A. Ali Kamboh (IntechOpen, 2019). Available at: http://dx.doi.org/10.5772/intechopen.82990

5. M. de Rojas, C. Riazzo, R. Callejon, D. Guevara, and C. Cutillas, "Molecular Study on Three Morphotypes of *Demodex* Mites (Acarina: Demodicidae) From Dogs," *Parasitology Research* 111 (2012): 2165–2172.

6. J. N. Izdebska and L. Rolbiecki, "The Status of *Demodex cornei*: Description of the Species and Developmental Stages, and Data on Demodecid Mites in the Domestic Dog *Canis lupus familiaris*," *Medical and Veterinary Entomology* 32 (2018): 346–357.

7. M. A. Milosevic, L. A. Frank, R. A. Brahmbhatt, and S. A. Kania, "PCR Amplification and DNA Sequencing of *Demodex injai* From Otic Secretions of a Dog," *Veterinary Dermatology* 24 (2013): 286-e66.

8. N. Sastre, I. Ravera, S. Villanueva, et al., "Phylogenetic Relationships in Three Species of Canine *Demodex* Mite Based on Partial Sequences of Mitochondrial 16S rDNA," *Veterinary Dermatology* 23 (2012): 509-e101.

9. D. G. Bowden, C. A. Outerbridge, M. B. Kissel, J. N. Baron, and S. D. White, "Canine Demodicosis: A Retrospective Study of a Veterinary Hospital Population in California, USA (2000–2016)," *Veterinary Dermatology* 29 (2018): 19-e0.

10. L. Ferrer, I. Ravera, and K. Silbermayr, "Immunology and Pathogenesis of Canine Demodicosis," *Veterinary Dermatology* 25 (2014): 427-e65.

11. S. K. Singh and U. Dimri, "The Immuno-Pathological Conversions of Canine Demodicosis," *Veterinary Parasitology* 203 (2014): 1–5.

12. S. K. Singh, U. Dimri, M. C. Sharma, et al., "The Role of Apoptosis in Immunosuppression of Dogs With Demodicosis," *Veterinary Immunology and Immunopathology* 144 (2011): 487–492.

13. P. Kumari, R. Nigam, S. Choudhury, et al., "*Demodex canis* Targets TLRs to Evade Host Immunity and Induce Canine Demodicosis," *Parasite Immunology* 40 (2018): e12509.

14. P. Kumari, R. Nigam, A. Singh, et al., "*Demodex canis* Regulates Cholinergic System Mediated Immunosuppressive Pathways in Canine Demodicosis," *Parasitology* 144 (2017): 1412–1416.

15. J. D. Plant, E. M. Lund, and M. Yang, "A Case-Control Study of the Risk Factors for Canine Juvenile-Onset Generalized Demodicosis in the USA," *Veterinary Dermatology* 22 (2011): 95–99.

16. J. L. Caswell, J. A. Yager, W. M. Parker, and P. F. Moore, "A Prospective Study of the Immunophenotype and Temporal Changes in the Histologic Lesions of Canine Demodicosis," *Veterinary Pathology* 34 (1997): 279–287.

17. M. J. Day, "An Immunohistochemical Study of the Lesions of Demodicosis in the Dog," *Journal of Comparative Pathology* 116 (1997): 203–216.

18. A. O. Felix, E. G. Guiot, M. Stein, S. R. Felix, E. F. Silva, and M. O. Nobre, "Comparison of Systemic Interleukin 10 Concentrations in Healthy Dogs and Those Suffering From Recurring and First Time *Demodex canis* Infestations," *Veterinary Parasitology* 193 (2013): 312–315.

19. T. Fukata, S. Aoki, H. Yoshikawa, Y. Kambayashi, K. Hitoh, and H. Kitagawa, "Significance of the CD4/CD8 Lymphocytes Ratio in Dogs Suffering From Demodicosis," *The Journal of Veterinary Medical Science* 58 (2005): 113–116.

20. M. Huisinga, K. Failing, and M. Reinacher, "MHC Class II Expression by Follicular Keratinocytes in Canine Demodicosis—An Immunohistochemical Study," *Veterinary Immunology and Immunopathology* 118 (2007): 210–220.

21. V. It, L. Barrientos, J. Lopez Gappa, et al., "Association of Canine Juvenile Generalized Demodicosis With the Dog Leukocyte Antigen System," *Tissue Antigens* 76 (2010): 67–70.

22. S. L. Lemarie and D. W. Horohov, "Evaluation of Interleukin-2 Production and Interleukin-2 Receptor Expression in Dogs With Generalized Demodicosis," *Veterinary Dermatology* 7 (1996): 213–219.

23. I. Ravera, D. Ferreira, L. S. Gallego, M. Bardagi, and L. Ferrer, "Serum Detection of IgG Antibodies Against *Demodex canis* by Western Blot in Healthy Dogs and Dogs With Juvenile Generalized Demodicosis," *Research in Veterinary Science* 101 (2015): 161–164.

24. A. K. S.-G. L. Rivas, L. Ferrer, and M. Bardagi, "Toll-Like Receptor 2 Is Overexpressed in Dogs With Demodicosis, Malassezia Dermatitis and Cutaneous Bacterial Infection," in *26th Annual Congress of the ECVD-ESVD*, (Valencia: Veterinary Dermatology, 2013), 377–397.

25. K. Tani, M. Morimoto, T. Hayashi, et al., "Evaluation of Cytokine Messenger RNA Expression in Peripheral Blood Mononuclear Cells From Dogs With Canine Demodicosis," *The Journal of Veterinary Medical Science* 64 (2002): 513–518.

26. G. F. Yarim, B. B. Yagci, M. Yarim, et al., "Serum Concentration and Skin Tissue Expression of Insulin-Like Growth Factor 2 in Canine Generalized Demodicosis," *Veterinary Dermatology* 26 (2015): 421-e99.

27. S. Y. Zheng, X. M. Hu, K. Huang, et al., "Proteomics as a Tool to Improve Novel Insights Into Skin Diseases: What We Know and Where We Should Be Going," *Frontiers in Surgery* 9 (2022): 1025557.

28. G. Fredman, L. Skov, M. Mann, and B. Dyring-Andersen, "Towards Precision Dermatology: Emerging Role of Proteomic Analysis of the Skin," *Dermatology* 238 (2022): 185–194.

29. J. Cox and M. Mann, "MaxQuant Enables High Peptide Identification Rates, Individualized p.p.b.—Range Mass Accuracies and Proteome-Wide Protein Quantification," *Nature Biotechnology* 26 (2008): 1367–1372.

30. S. Tyanova, T. Temu, P. Sinitcyn, et al., "The Perseus Computational Platform for Comprehensive Analysis of (Prote)omics Data," *Nature Methods* 13 (2016): 731–740.

31. S. Tyanova, T. Temu, and J. Cox, "The MaxQuant Computational Platform for Mass Spectrometry-Based Shotgun Proteomics," *Nature Protocols* 11 (2016): 2301–2319.

32. V. G. Tusher, R. Tibshirani, and G. Chu, "Significance Analysis of Microarrays Applied to the Ionizing Radiation Response," *Proceedings of the National Academy of Sciences of the United States of America* 98 (2001): 5116–5121.

33. Y. Perez-Riverol, J. Bai, C. Bandla, et al., "The PRIDE Database Resources in 2022: A Hub for Mass Spectrometry-Based Proteomics Evidences," *Nucleic Acids Research* 50 (2022): D543–D552.

34. Y. Zhou, B. Zhou, L. Pache, et al., "Metascape Provides a Biologist-Oriented Resource for the Analysis of Systems-Level Datasets," *Nature Communications* 10 (2019): 1523.

35. A. Krämer, J. Green, J. Pollard, Jr., and S. Tugendreich, "Causal Analysis Approaches in Ingenuity Pathway Analysis," *Bioinformatics* 30 (2014): 523–530.

36. Y. Benjamini and Y. Hochberg, "Controlling the False Discovery Rate—A Practical and Powerful Approach to Multiple Testing," *Journal of the Royal Statistical Society: Series B: Methodological* 57 (1995): 289–300.

37. C. A. Schneider, W. S. Rasband, and K. W. Eliceiri, "NIH Image to ImageJ: 25 Years of Image Analysis," *Nature Methods* 9 (2012): 671–675.

38. F. Varghese, A. B. Bukhari, R. Malhotra, and A. De, "IHC Profiler: An Open Source Plugin for the Quantitative Evaluation and Automated Scoring of Immunohistochemistry Images of Human Tissue Samples," *PLoS One* 9 (2014): e96801.

39. K. Weke, S. Kote, J. Faktor, et al., "DIA-MS Proteome Analysis of Formalin-Fixed Paraffin-Embedded Glioblastoma Tissues," *Analytica Chimica Acta* 1204 (2022): 339695.

40. A. J. Nwosu, S. A. Misal, T. Truong, et al., "In-Depth Mass Spectrometry-Based Proteomics of Formalin-Fixed, Paraffin-Embedded Tissues With a Spatial Resolution of 50–200 μm," *Journal of Proteome Research* 21 (2022): 2237–2245.

41. M. Acosta-Martinez and M. Z. Cabail, "The PI3K/Akt Pathway in Meta-Inflammation," *International Journal of Molecular Sciences* 23 (2022): 15330.

42. E. Vergadi, E. Ieronymaki, K. Lyroni, K. Vaporidi, and C. Tsatsanis, "Akt Signaling Pathway in Macrophage Activation and M1/M2 Polarization," *Journal of Immunology* 198 (2017): 1006–1014.

43. J. Holbrook, S. Lara-Reyna, H. Jarosz-Griffiths, and M. McDermott, "Tumour Necrosis Factor Signalling in Health and Disease," *F1000Research* 8 (2019): 1–12.

44. A. Krämer, J. N. Billaud, S. Tugendreich, D. Shiffman, M. Jones, and J. Green, "The Coronavirus Network Explorer: Mining a Large-Scale Knowledge Graph for Effects of SARS-CoV-2 on Host Cell Function," *BMC Bioinformatics* 22 (2021): 229.

45. C. N. Correia, G. P. McHugo, J. A. Browne, et al., "High-Resolution Transcriptomics of Bovine Purified Protein Derivative-Stimulated Peripheral Blood From Cattle Infected With *Mycobacterium bovis* Across an Experimental Time Course," *Tuberculosis* 136 (2022): 102235.

46. T. Adomavicius, M. Guaita, Y. Zhou, et al., "The Structural Basis of Translational Control by eIF2 Phosphorylation," *Nature Communications* 10 (2019): 2136.

47. R. A. Saxton and D. M. Sabatini, "mTOR Signaling in Growth, Metabolism, and Disease," *Cell* 168 (2017): 960–976.

48. M. D. Dennis, L. S. Jefferson, and S. R. Kimball, "Role of p70S6K1-Mediated Phosphorylation of eIF4B and PDCD4 Proteins in the Regulation of Protein Synthesis," *The Journal of Biological Chemistry* 287 (2012): 42890–42899.

49. T. J. Rios-Fuller, M. Mahe, B. Walters, et al., "Translation Regulation by eIF2α Phosphorylation and mTORC1 Signaling Pathways in Non-Communicable Diseases (NCDs)," *International Journal of Molecular Sciences* 21 (2020): 5301.

50. S. Kim, Y. Joe, Y. J. Surh, and H. T. Chung, "Differential Regulation of Toll-Like Receptor-Mediated Cytokine Production by Unfolded Protein Response," *Oxidative Medicine and Cellular Longevity* 2018 (2018): 9827312.

51. D. Geng, L. Zheng, R. Srivastava, N. Asprodites, C. Velasco-Gonzalez, and E. Davila, "When Toll-Like Receptor and T-Cell Receptor Signals Collide: A Mechanism for Enhanced CD8 T-Cell Effector Function," *Blood* 116 (2010): 3494–3504.

52. C. Buerger, "Epidermal mTORC1 Signaling Contributes to the Pathogenesis of Psoriasis and Could Serve as a Therapeutic Target," *Frontiers in Immunology* 9 (2018): 2786.

53. A. S. Naeem, C. Tommasi, C. Cole, et al., "A Mechanistic Target of Rapamycin Complex 1/2 (mTORC1)/V-Akt Murine Thymoma Viral Oncogene Homolog 1 (AKT1)/Cathepsin H Axis Controls Filaggrin Expression and Processing in Skin, a Novel Mechanism for Skin Barrier Disruption in Patients With Atopic Dermatitis," *The Journal of Allergy and Clinical Immunology* 139 (2017): 1228–1241.

54. K. Park, S. E. Lee, K. O. Shin, and Y. Uchida, "Insights Into the Role of Endoplasmic Reticulum Stress in Skin Function and Associated Diseases," *The FEBS Journal* 286 (2019): 413–425.

55. V. B. Stevenson, S. Klahn, T. LeRoith, and W. R. Huckle, "Canine Melanoma: A Review of Diagnostics and Comparative Mechanisms of Disease and Immunotolerance in the Era of the Immunotherapies," *Frontiers in Veterinary Science* 9 (2022): 1046636.

56. E. Beebe, A. Pöschel, L. Kunz, et al., "Proteomic Profiling of Canine Fibrosarcoma and Adjacent Peritumoral Tissue," *Neoplasia* 35 (2023): 100858.

57. B. C. Melnik, "Endoplasmic Reticulum Stress: Key Promoter of Rosacea Pathogenesis," *Experimental Dermatology* 23 (2014): 868–873.

58. P. A. Kelly, J. Browne, S. Peters, et al., "Gene Expression Analysis of Canine Demodicosis; a Milieu Promoting Immune Tolerance," *Veterinary Parasitology* 319 (2023): 109954.

59. G. Di Conza and P. C. Ho, "ER Stress Responses: An Emerging Modulator for Innate Immunity," *Cells* 9 (2020): 695.

60. J. R. Cubillos-Ruiz, S. E. Bettigole, and L. H. Glimcher, "Tumorigenic and Immunosuppressive Effects of Endoplasmic Reticulum Stress in Cancer," *Cell* 168 (2017): 692–706.

61. R. C.-R. Juan, M. Eslam, and C. R. Paulo, "Unfolding Anti-Tumor Immunity: ER Stress Responses Sculpt Tolerogenic Myeloid Cells in Cancer," *Journal for Immunotherapy of Cancer* 5 (2017): 5.

62. Y.-P. Liu, L. Zeng, A. Tian, et al., "Endoplasmic Reticulum Stress Regulates the Innate Immunity Critical Transcription Factor IRF3," *Journal of Immunology* 189 (2012): 4630–4639.

63. K. E. Hurst, K. A. Lawrence, M. T. Essman, Z. J. Walton, L. R. Leddy, and J. E. Thaxton, "Endoplasmic Reticulum Stress Contributes to Mitochondrial Exhaustion of CD8(+) T Cells," *Cancer Immunology Research* 7 (2019): 476–486.

64. K. Kemp and C. Poe, "Stressed: The Unfolded Protein Response in T Cell Development, Activation, and Function," *International Journal of Molecular Sciences* 20 (2019): 1792.

65. F. Veglia, E. Sanseviero, and D. I. Gabrilovich, "Myeloid-Derived Suppressor Cells in the Era of Increasing Myeloid Cell Diversity," *Nature Reviews. Immunology* 21 (2021): 485–498.

66. L. N. Raines, H. Zhao, Y. Wang, et al., "PERK Is a Critical Metabolic Hub for Immunosuppressive Function in Macrophages," *Nature Immunology* 23 (2022): 431–445.

67. A. C. Costa-da-Silva, D. O. Nascimento, J. R. M. Ferreira, et al., "Immune Responses in Leishmaniasis: An Overview," *Tropical Medicine and Infectious Diseases* 7 (2022): 54.

68. J. M. Hu, K. Liu, J. H. Liu, et al., "CD163 as a Marker of M2 Macrophage, Contribute to Predict Aggressiveness and Prognosis of Kazakh Esophageal Squamous Cell Carcinoma," *Oncotarget* 8 (2017): 21526–21538.

69. I. Kwiecień, M. Polubiec-Kownacka, D. Dziedzic, D. Wołosz, P. Rzepecki, and J. Domagała-Kulawik, "CD163 and CCR7 as Markers for Macrophage Polarization in Lung Cancer Microenvironment," *Central European Journal of Immunology* 44 (2019): 395–402.

70. S. Prokop, F. L. Heppner, H. H. Goebel, and W. Stenzel, "M2 Polarized Macrophages and Giant Cells Contribute to Myofibrosis in Neuromuscular Sarcoidosis," *The American Journal of Pathology* 178 (2011): 1279–1286.

71. R. W. Hallowell, S. L. Collins, J. M. Craig, et al., "mTORC2 Signalling Regulates M2 Macrophage Differentiation in Response to Helminth Infection and Adaptive Thermogenesis," *Nature Communications* 8 (2017): 14208.

72. S. Kadomoto, K. Izumi, and A. Mizokami, "Macrophage Polarity and Disease Control," *International Journal of Molecular Sciences* 23 (2022): 144.

73. A. L. Farrow, T. Rana, M. K. Mittal, S. Misra, and G. Chaudhuri, "Leishmania-Induced Repression of Selected Non-Coding RNA Genes Containing B-Box Element at Their Promoters in Alternatively Polarized M2 Macrophages," *Molecular and Cellular Biochemistry* 350 (2011): 47–57.

74. F. Tomiotto-Pellissier, B. T. S. Bortoleti, J. P. Assolini, et al., "Macrophage Polarization in Leishmaniasis: Broadening Horizons," *Frontiers in Immunology* 9 (2018): 2529.

75. X. Ding, W. Bloch, S. Iden, et al., "mTORC1 and mTORC2 Regulate Skin Morphogenesis and Epidermal Barrier Formation," *Nature Communications* 7 (2016): 13226.

76. J. Wang, B. Cui, Z. Chen, and X. Ding, "The Regulation of Skin Homeostasis, Repair and the Pathogenesis of Skin Diseases by Spatiotemporal Activation of Epidermal mTOR Signaling," *Frontiers in Cell and Development Biology* 10 (2022): 950973.

77. P. A. Kelly, J. S. McKay, D. Maguire, et al., "A Retrospective Study of Cases of Canine Demodicosis Submitted to a Commercial Diagnostic Laboratory Servicing the United Kingdom and Ireland (2017–2018): Part 1—Signalment, Lesion Distribution, Treatments, and Concurrent Diseases," *Research in Veterinary Science* 153 (2022): 99–104.

78. Z. Deng, M. Chen, Y. Liu, et al., "A Positive Feedback Loop Between mTORC1 and Cathelicidin Promotes Skin Inflammation in Rosacea," *EMBO Molecular Medicine* 13 (2021): e13560.

79. Q. Peng, K. Sha, Y. Liu, et al., "mTORC1-Mediated Angiogenesis Is Required for the Development of Rosacea," *Frontiers in Cell and Development Biology* 9 (2021): 751785.

80. H. Wang, L. Duan, Z. Zou, et al., "Activation of the PI3K/Akt/mTOR/p70S6K Pathway Is Involved in S100A4-Induced Viability and Migration in Colorectal Cancer Cells," *International Journal of Molecular Sciences* 11 (2014): 841–849.

81. K. Tengvall, K. Bergvall, M. Olsson, et al., "Transcriptomes From German Shepherd Dogs Reveal Differences in Immune Activity Between Atopic Dermatitis Affected and Control Skin," *Immunogenetics* 72 (2020): 315–323.

82. L. F. Mellor, N. Gago-Lopez, L. Bakiri, et al., "Keratinocyte-Derived S100A9 Modulates Neutrophil Infiltration and Affects Psoriasis-Like Skin and Joint Disease," *Annals of the Rheumatic Diseases* 81 (2022): 1400–1408.

83. R. W. Sprung, J. W. C. Brock, J. P. Tanksley, et al., "Equivalence of Protein Inventories Obtained From Formalin-Fixed Paraffin-Embedded and Frozen Tissue in Multidimensional Liquid Chromatography-Tandem Mass Spectrometry Shotgun Proteomic Analysis," *Molecular & Cellular Proteomics* 8 (2009): 1988–1998.

84. B. L. Hood, M. M. Darfler, T. G. Guiel, et al., "Proteomic Analysis of Formalin-Fixed Prostate Cancer Tissue," *Molecular & Cellular Proteomics* 4 (2005): 1741–1753.

85. T. Guo, W. Wang, P. A. Rudnick, et al., "Proteome Analysis of Microdissected Formalin-Fixed and Paraffin-Embedded Tissue Specimens," *The Journal of Histochemistry and Cytochemistry* 55 (2007): 763–772.

Supporting Information

Additional supporting information can be found online in the Supporting Information section.